

Content from this work may be used under the terms of the CC BY 3.0 licence (© 2021). Any distribution of this work must maintain attribution to the author(s), title of the work, publisher, and DOI

GENERATING 510 MW OF X-BAND POWER FOR STRUCTURE-BASED WAKEFIELD ACCELERATION USING A METAMATERIAL-BASED POWER EXTRACTOR

J. Picard*, I. Mastovsky, M. A. Shapiro, R. J. Temkin
Massachusetts Institute of Technology, Cambridge, MA, USA
X. Lu¹, Northern Illinois University, DeKalb, IL, USA
M. Conde, D. S. Doran, J. G. Power, J. Shao, E. E. Wisniewski
Argonne National Laboratory, Lemont, IL, USA
C. Jing, Euclid Techlabs LLC, Solon, OH, USA
¹also at Argonne National Laboratory, Lemont, IL, USA

Abstract

We present our recent results generating 510 MW of power at 11.7 GHz using a metamaterial-based metallic power extractor for structure-based wakefield acceleration (SWFA). Implementing metamaterials in a power extractor design allows the structure to overcome some of the challenges faced by other SWFA techniques. Two previous experiments, Stage 1 in 2018 and Stage 2 in 2019, have successfully demonstrated the functionality of this approach by generating high power pulses using the 65 MeV electron beam at the Argonne Wakefield Accelerator (AWA) facility. Here, we discuss the design and results of the Stage 3 experiment. The Stage 3 design includes significant improvements to increase output power, employing an all-copper structure, fully-symmetric coupler design, and breakdown risk-reduction treatment.

INTRODUCTION

Structure-based wakefield acceleration (SWFA) holds great promise in the future of high-gradient particle acceleration [1, 2]. SWFA is a novel acceleration scheme in which high-charge drive bunches are passed through a structure to produce a high-intensity wakefield. This wakefield can then be used to accelerate a low-charge witness bunch in the same beamline (collinear acceleration) or passed to a separate acceleration beamline (two-beam acceleration, or TBA). In the case of TBA, a specific, dedicated structure is utilized to efficiently extract power from the drive bunch: the power extractor. Various metallic and dielectric power extractor designs have been demonstrated [2–8]. Because metamaterials have been shown to be a promising candidate for generating high power microwaves [9–15], MIT has developed a power extractor design using a custom metamaterial, termed the “wagon wheel metamaterial.” This structure presents several advantages over existing power extractor designs, including a rugged metal construction, a high degree of flexibility in parameter space, and a simultaneously high group velocity and shunt impedance [5, 16].

Two exploded unit cells of wagon wheel metamaterial are pictured in Fig. 1. Each cell consists of one structure

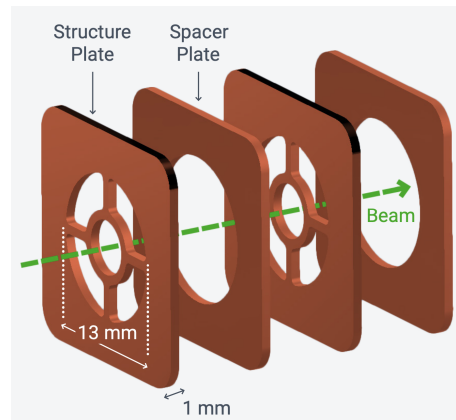


Figure 1: Exploded view of two wagon wheel metamaterial unit cells.

plate and one spacer plate, each 1 mm in thickness. The resulting macroscopic metamaterial is subwavelength, which can be seen by comparing the 2 mm period with the ≈ 20 mm wavelength at X-band. The simulated dispersion curve of the material can be seen in Fig. 2. When a high-energy electron bunch is passed through the center, the bunch radiates in the backward direction as reverse Cherenkov radiation at the 11.7 GHz interaction frequency [17]. This is reflected in the negative slope of the dispersion curve, where the group velocity is $v_g = -0.155c$. This fundamental mode has a high r/Q of 20.2 k Ω /m.

This metamaterial has been implemented in two previous power extractor experiments: Stage 1 with 40 cells in 2018 [16], and Stage 2 with 100 cells in 2019 [18]. Based on these experiments, several major improvements were made in developing the Stage 3 design and are discussed in the following section. All three experiments have been tested at the 65 MeV Argonne Wakefield Accelerator (AWA) at Argonne National Lab with trains of between one and eight electron bunches with charge levels up to 280 nC total. Bunches are generated at the 1.3 GHz frequency of the L-band accelerator.

* jpicard@mit.edu

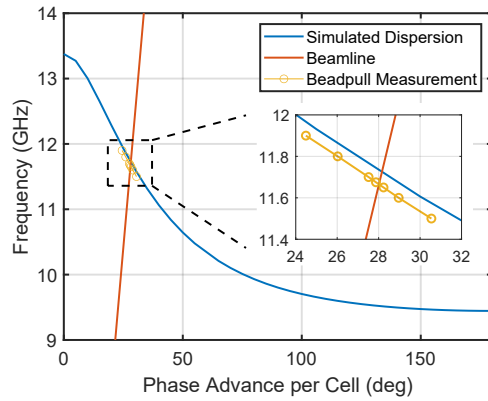


Figure 2: Comparison of simulated and experimentally-measured dispersion curves for the wagon wheel metamaterial.

STAGE 3 DESIGN

The fully-assembled Stage 3 experiment can be seen in Fig. 3. In aggregate, for a given electron bunch, the following improvements increase the power generation by a factor of ≈ 1.7 over the Stage 2 experiment.

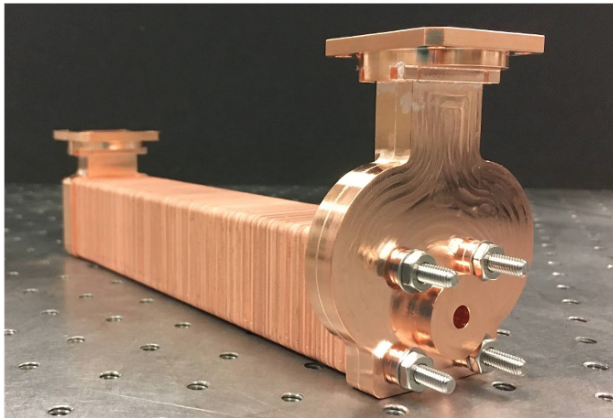


Figure 3: Fully-assembled Stage 3 power extractor prior to vacuum installation.

All-Copper Construction

One major improvement made in the Stage 3 experiment was to fabricate the metamaterial plates from OFHC copper to reduce RF loss. Stainless steel (SST) was used in the Stage 1 and 2 experiments to reduce the potential for damage during handling and assembly, at the cost of lower conductivity. In the Stage 2 experiment, cold tests showed that α , the field decay per unit length in the structure, was 3.0 m^{-1} . This corresponds to an insertion loss of -6.3 dB at 11.7 GHz , as seen in Fig. 4. By fabricating the structure plates from OFHC copper α was reduced to 0.33 m^{-1} and the insertion loss was reduced to -1.3 dB . This allows the all-copper structure to generate a factor of ≈ 1.5 higher power from a given bunch than a structure manufactured from SST. For example, from a 20 nC bunch, the all-copper structure

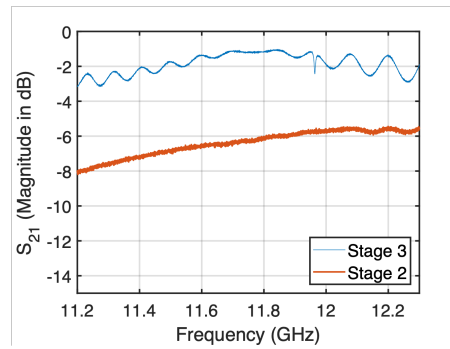


Figure 4: Comparison of S_{21} measurements showing the reduction in transmission loss in the Stage 3 experiment.

would generate 3.1 MW of power versus 2.0 MW from the SST structure.

Symmetric High Power Coupler

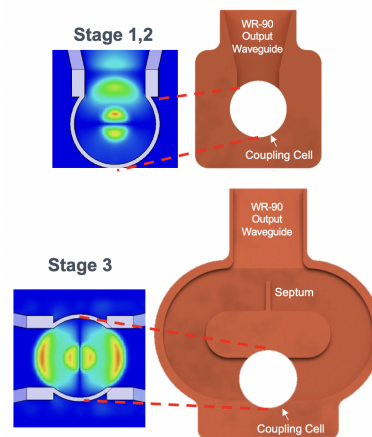


Figure 5: The asymmetric coupler used in Stage 1 and 2 (top), which caused a transverse kick to the beam, was symmetrized in the Stage 3 experiment (bottom).

Power is extracted from the metamaterial cells using a set of couplers: the "forward" coupler, which couples the small amount of power travelling in the forward direction, and the "backward" coupler, which couples the main high power pulse propagating backwards. In the Stage 1 and 2 experiments, both couplers were of the same design, see Fig. 5, top. The vertical asymmetry in the coupler design generated a correspondingly asymmetric mode in the coupling cell at the high-power 11.7 GHz frequency. As a result, bunches entering the structure received a transverse kick. For example, in a train of eight 40 nC bunches, simulations show that after high power levels are generated in the structure by earlier bunches, this kick can be large enough to introduce a trajectory angle of 0.5° for the later bunches. This effect both reduces the efficiency of power generation and makes beam alignment and transmission more challenging.

The Stage 3 experiment incorporates a symmetric coupler design for the high-power backward coupler, shown in Fig. 5, bottom, in which the coupling cell has been symmetrized

Content from this work may be used under the terms of the CC BY 3.0 licence (© 2021). Any distribution of this work must maintain attribution to the author(s), title of the work, publisher, and DOI

using a racetrack-style scheme [19]. The resulting mode is now bidirectionally symmetric, which eliminates the transverse kick and maintains an on-axis bunch trajectory. This increases the power output by approximately 15% over the non-symmetric coupler design: the all-copper structure with symmetric coupler would generate 3.5 MW of power from a 20 nC bunch in comparison to 3.1 MW with the asymmetric design. The forward coupler remains asymmetric because of the low power level at this coupler and the consequent negligible effect of the asymmetry on power generation.

Surface Treatment of Metamaterial Plates

The metamaterial plates were fabricated using wire-EDM. Despite careful manufacturing, defects (generally scratches and dents) were left on the plate surface. Wire-EDM also leaves particularly sharp corners along the cutting edge. To minimize the chance that either damage sites or sharp corners would initiate breakdown during experiment, we used dilute Citranox (acid) baths to lightly etch the surface of the plates. Both visible microscope and SEM images show that this calibrated processing successfully smoothed both the plate damage and the sharp corner features. In addition to this treatment, visible-light breakdown diagnostics were implemented to monitor for breakdowns in the output couplers.

EXPERIMENTAL RESULTS

Cold tests performed at MIT and AWA show excellent agreement with simulation, as shown in Fig. 6. This agreement indicates both that simulations modeled the copper conductivity well and that fabrication tolerances were met. A beadpull setup was used to experimentally measure the dispersion curve of the fabricated structure [20]. The results are shown in the inset of Fig. 2 and indicate that the interaction frequency is 11.675 GHz - within the tunable range of the AWA bunch train separation.

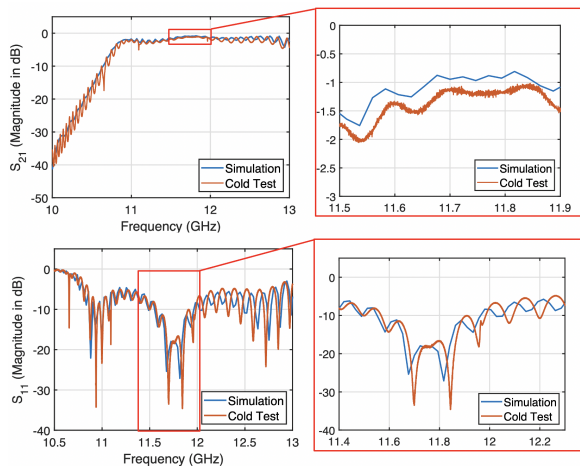


Figure 6: Cold Test results showing excellent agreement with simulation.

The Stage 3 structure produced 510 MW during hot testing with the 65 MeV electron beam at AWA, as seen in Fig. 7.

This power was generated from an 8-bunch train with total charge of 280 nC, and represents the highest power output by a structure-based power extractor at AWA to-date [21]. The corresponding on-axis accelerating gradient has been calculated to be 128 MV/m. The frequency of the generated RF was 11.675 GHz, in excellent agreement with a PIC simulation and the beadpull measurement. No evidence of breakdown was present in the visible light diagnostics.

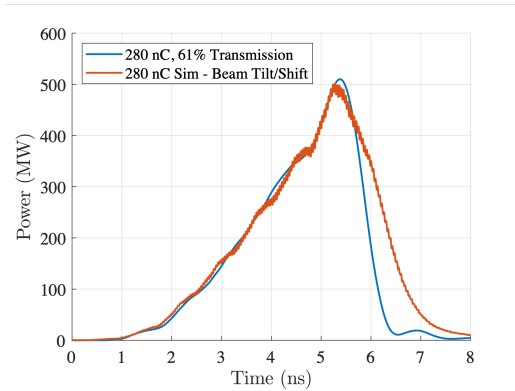


Figure 7: The Stage 3 experiment generated 510 MW of power and show excellent agreement with simulations that take into account observed bunch offsets.

The output power from the Stage 3 experiment was limited by two factors: available charge and small tilts/offsets in the incident bunch trajectory. Beam images before the structure indicate that bunches 2-8 of the eight bunch train were spatially shifted by a distance on the order of the bunch diameter. This bunch trajectory error is believed to be due to undamped transverse wakes in the 65 MeV accelerator and results in reduced power generation by the structure. Using measurements from the beam imaging cameras, revised PIC simulations were run to take into account this effect. The results, overlaid with experiment in Fig. 7, show excellent agreement with experimental data. CST particle-in-cell simulations show that, without this tilt/offset of the bunches, a 360 nC train of 8 bunches, which is the nominal capability of the AWA, is capable of generating over 1.1 GW of power.

CONCLUSION

The Stage 3 metamaterial-based power extractor successfully generated 510 MW of power at 11.7 GHz at the 65 MeV Argonne Wakefield Accelerator. This represents the highest power level generated by a structure-based power extractor. These results were made possible by the improvements implemented in the Stage 3 design, including an all-copper construction, symmetric high-power output coupler, and acid etching treatment to reduce possible breakdown-initiation sites on the metamaterial plates.

ACKNOWLEDGEMENTS

The work was funded by the Department of Energy under contracts DE-SC0011556 and DE-AC02-06CH11357.

REFERENCES

- [1] B. Cros and P. Muggli, "Towards a Proposal for an Advanced Linear Collider Report", presented at Advanced and Novel Accelerators for High Energy Physics Roadmap Workshop", Geneva, Switzerland, Apr. 2017, unpublished.
- [2] C. Jing *et al.*, "Experimental demonstration of wakefield acceleration in a tunable dielectric loaded accelerating structure," *Phys. Rev. Lett.*, vol. 106, p. 164 802, Apr. 2011, doi:10.1103/PhysRevLett.106.164802
- [3] J. Shao *et al.*, "Development and high-power testing of an X-band dielectric-loaded power extractor," *Phys. Rev. Accel. Beams*, vol. 23, p. 011 301, Jan. 2020, doi:10.1103/PhysRevAccelBeams.23.011301
- [4] R. Corsini, "Final Results From the CLIC Test Facility (CTF3)," pp. 1269–1274, May 2017, doi:10.18429/JACoW-IPAC2017-TUZB1
- [5] F. Gao *et al.*, "Design and testing of a 7.8 GHz power extractor using a cylindrical dielectric-loaded waveguide," *Phys. Rev. Accel. Beams*, vol. 11, p. 041 301, Apr. 2008, doi:10.1103/PhysRevSTAB.11.041301
- [6] G. Andonian *et al.*, "Dielectric wakefield acceleration of a relativistic electron beam in a slab-symmetric dielectric lined waveguide," *Phys. Rev. Lett.*, vol. 108, p. 244 801, Jun. 2012, doi:10.1103/PhysRevLett.108.244801
- [7] M. Peng *et al.*, "Generation of high power short RF pulses using an X-band metallic power extractor driven by high charge multi-bunch train," in *Proc. 10th International Particle Accelerator Conference (IPAC'19)*, Melbourne, Australia, Melbourne, Australia, pp. 734–737, doi:10.18429/JACoW-IPAC2019-MOPRB069
- [8] B. D. O'Shea *et al.*, "Observation of acceleration and deceleration in giga-electron-volt-per-metre gradient dielectric wakefield accelerators," *Nat Commun*, vol. 7, p. 12 763, 2016, doi:10.1038/ncomms12763
- [9] J. S. Hummelt, X. Lu, H. Xu, I. Mastovsky, M. A. Shapiro, and R. J. Temkin, "Coherent cherenkov-cyclotron radiation excited by an electron beam in a metamaterial waveguide," *Phys. Rev. Lett.*, vol. 117, p. 237 701, Dec. 2016, doi:10.1103/PhysRevLett.117.237701
- [10] X. Lu, J. C. Stephens, I. Mastovsky, M. A. Shapiro, and R. J. Temkin, "High power long pulse microwave generation from a metamaterial structure with reverse symmetry," *Physics of Plasmas*, vol. 25, no. 2, p. 023 102, 2018, doi:10.1063/1.5016545
- [11] S. Antipov *et al.*, "Observation of wakefield generation in left-handed band of metamaterial-loaded waveguide," *Journal of Applied Physics*, vol. 104, no. 1, p. 014 901, 2008, doi:10.1063/1.2948929
- [12] S. Antipov, L. Spentzouris, W. Liu, W. Gai, and J. G. Power, "Wakefield generation in metamaterial-loaded waveguides," *Journal of Applied Physics*, vol. 102, no. 3, p. 034 906, 2007, doi:10.1063/1.2767640
- [13] T. Rowe, N. Behdad, and J. H. Booske, "Metamaterial-enhanced resistive wall amplifier design using periodically spaced inductive meandered lines," *IEEE Transactions on Plasma Science*, vol. 44, no. 10, pp. 2476–2484, 2016, doi:10.1109/TPS.2016.2599144
- [14] S. Antipov *et al.*, "Observation of wakefield generation in left-handed band of metamaterial-loaded waveguide," *Journal of Applied Physics*, vol. 104, no. 1, p. 014 901, 2008, doi:10.1063/1.2948929
- [15] Z. Duan *et al.*, "Metamaterial-inspired vacuum electron devices and accelerators," *IEEE Transactions on Electron Devices*, vol. 66, no. 1, pp. 207–218, 2019, doi:10.1109/TED.2018.2878242
- [16] X. Lu *et al.*, "Generation of high-power, reversed-cherenkov wakefield radiation in a metamaterial structure," *Phys. Rev. Lett.*, vol. 122, p. 014 801, Jan. 2019, doi:10.1103/PhysRevLett.122.014801
- [17] H. Chen and M. Chen, "Flipping photons backward: Reversed cherenkov radiation," *Materials Today*, vol. 14, no. 1, pp. 34–41, 2011, doi:10.1016/S1369-7021(11)70020-7
- [18] X. Lu *et al.*, "Coherent high-power rf wakefield generation by electron bunch trains in a metamaterial structure," *Applied Physics Letters*, vol. 116, no. 26, p. 264 102, 2020, doi:10.1063/5.0012671
- [19] Z. Li *et al.*, "Coupler design for the lcls injector s-band structures," in *Proc. 21st Particle Accelerator Conf. (PAC'05)*, Knoxville, TN, USA, May 2005, paper TPPT031, pp. 2176–2178.
- [20] C. Steele, "A nonresonant perturbation theory," *IEEE Transactions on Microwave Theory and Techniques*, vol. 14, no. 2, pp. 70–74, 1966, doi:10.1109/TMTT.1966.1126168
- [21] J. Power, "High gradient research activities at AWA: The short pulse regime," unpublished.